

CHAPTER IV

RESULTS AND DISCUSSION

4.1 Water Content Analysis

Referring to many literatures that suggest preheating of the powder form zeolite at 400°C for 12 hours before use and also in accordance with the previous work last year that preheated zeolite to 350°C, in this work, preheating of the pellet commercial zeolite containing some amount of binder was conducted.

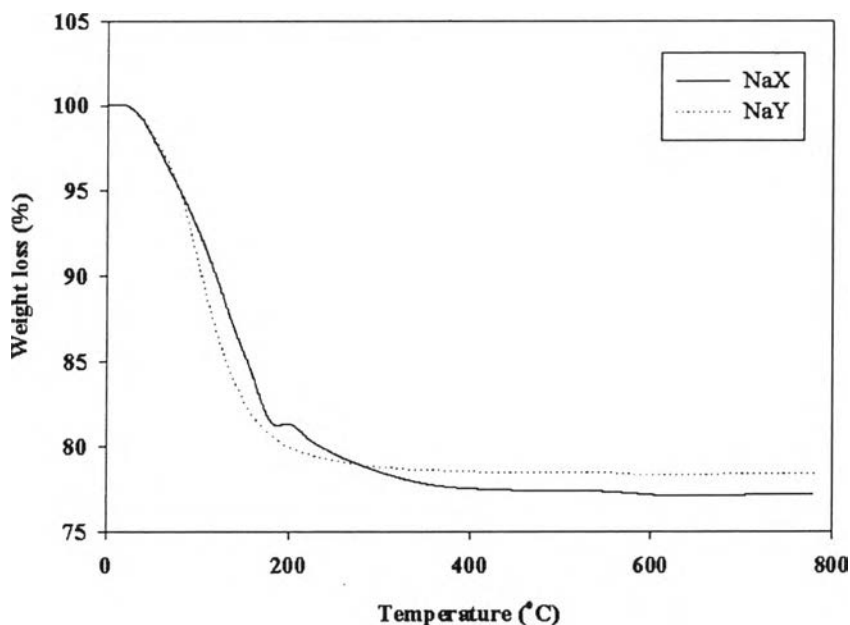


Figure 4.1 Thermogram of commercial zeolites

The resulted thermogram (Figure 4.1) shows the weight loss in percent with respect to temperature. The weight loss of both NaX and NaY decreased rapidly when the temperature reached around 100°C and became constant around 400°C. At around 100°C (boiling point of water), water molecules desorbed. Based on original weights and weight loss calculation, the total amounts of water adsorbed on zeolite X and Y were found to be 22.58% and 21.26%, respectively. This is consistent with the

fact that, the lower Si/Al ratio (corresponding to higher number of Na counter cation which is adsorption site) of NaX results in higher adsorption of water molecules. Therefore, the water content in the zeolites was controlled before use by preheating in the oven at a constant heating rate of 10°C/min from room temperature to 400 °C and held constant for 12 hours.

4.2 Quantity of Appropriate Zeolite Adsorbent

As most experiments were planned to employ solutions of 2000 ppb mercury, while keeping Hg level in the final solution low but measurable, therefore, the appropriate mass of adsorbent for 2000 ppb solution of mercury need to be determined. Different quantity of adsorbent was loaded, i.e. 0.1, 0.2, 0.3, 0.4 and 0.5 g (Figure 4.2).

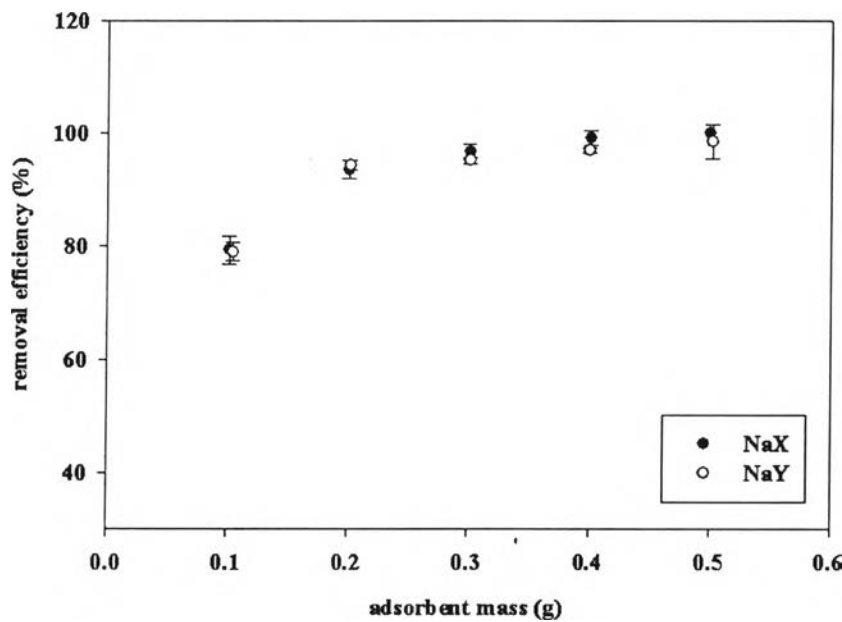


Figure 4.2 Adsorption efficiency of the zeolites at 30°C (2000 ppb of DPM in n-heptane)

Referring to chapter three, the experiments were conducted in batch system by adding up 15 ml of sample solution into a 15 ml plastic bottle, shaken for at least

7 hours to reach its equilibrium at room temperature (The kinetic results from the previous work indicate that the adsorption of DPM by NaX and NaY reaches equilibrium at around 7 hours.).

The rapid increase of removal efficiency was obtained from 0.1 g of adsorbent to 0.2 g of adsorbent. To allow for measurable concentration of Hg remaining in the sample solution, 0.1 g of adsorbent was chosen for most of the following experiment.

4.3 Effect of Water Content in the Zeolite on the Adsorption of DPM

The role of water content in zeolite was to increase the selectivity. In this work, the selectivity of DPM molecule to NaX and NaY was determined. Referring to the chapter three, the weighed adsorbent was exposed to air to adsorb moisture until the desired water content was reached, i.e. at 1, 3, 5 and 7%. The result is shown in Figure 4.3.

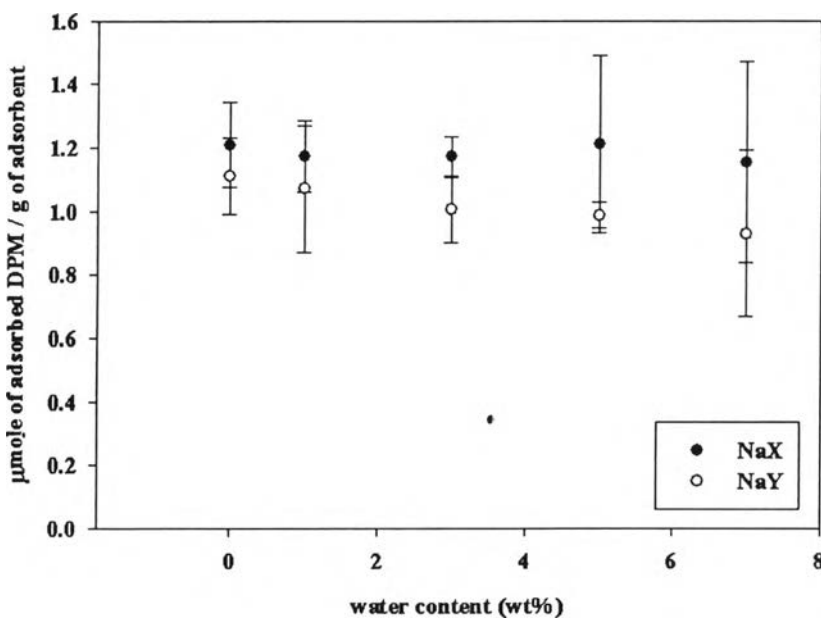
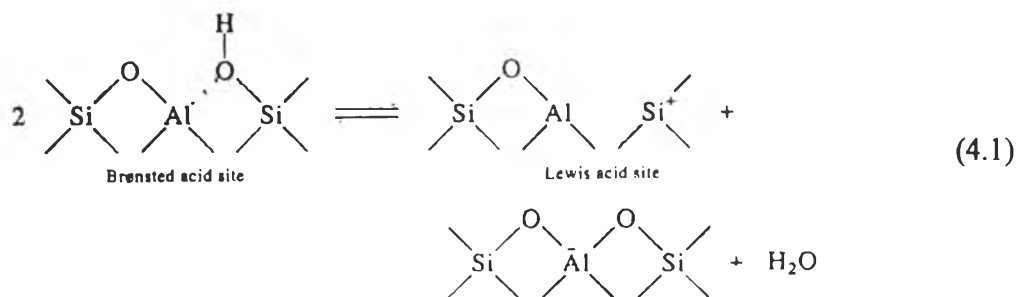


Figure 4.3 Effect of water content in the zeolites (2000 ppb of DPM in n-heptane)

The adsorption capacity of NaX was found to be higher than the capacity of NaY at the same filling amount of water. As the filling of water increased, the adsorption capacity of both zeolites tended to be lower. At 0% water, NaX, which possessed higher acidity, adsorbed more DPM than NaY.

When water molecule is added to the framework, it leads to the formation of Brønsted acid site as the followings (Gates, 1991):



From the stoichiometry, one Lewis acid site is formed from two Brønsted acid sites, so, the adsorbent that has high content of Al like NaX can form higher numbers of Brønsted sites compared with NaY that has lower Al content. Therefore, the adsorption capacity of NaX is higher than of NaY. The lowering of the adsorption capacity cause by DPM molecule does not selectively adsorb onto Brønsted acid site. However, in this work, percent decrease of adsorption capacity of NaX and NaY at 7% of water content were found, and that of NaX was lower than NaY, at $5\pm8\%$ and $20\pm8\%$, respectively. The water content in the range of 0-7% did not effect adsorption capacity of NaX while the adsorption capacity of NaY was significantly affected. Thus, physical properties, especially pore volume were taken into consideration. The pore volume of NaX and NaY were 0.25 and $0.27 \text{ cm}^3/\text{g}$, respectively (Table 3.1). Moïse *et al.*, (2001) proposed the adsorption mechanisms of water molecule onto BaX and BaY zeolite so called three-step mechanism; adsorption on compensating cation, formation of a monolayer on the walls and multilayer adsorption in the cavity (capillary condensation). Therefore, the more significant decrease of adsorption capacity of NaY could be caused by co-effect of capillary condensation of water molecule as the pore volume of NaY was higher than

that of NaX resulting in easier condensation of water. The selectivity of DPM to NaX and NaY was also calculated in Table 4.1.

Table 4.1 Selectivity of diphenylmercury (2000 ppb of DPM in n-heptane)

water content (wt%)	selectivity	
	NaX/NaY	NaY/NaX
0	2.12	0.47
1	2.16	0.46
3	3.31	0.30
5	5.29	0.18
7	3.19	0.31

4.4 Adsorption Isotherm of DPM in n-Heptane

The result obtained for NaX is shown in Figure 4.4. The adsorption isotherms of NaX were performed at three temperatures, 30, 40 and 50°C. The experiment could not be done at temperature higher than 50°C as large variation of the results was observed because the bottle used in the experiment became soft and collapse resulted in spillage of water (in the water bath) into the bottle and covered the adsorbent. The adsorption isotherm at lower temperature was higher than at higher temperature. The adsorption isotherms obtained for NaY also shows the same trend (Figure 4.5), i.e. the higher the temperature, the lower the adsorption. Thus, adsorbed molecules could be easily desorbed by increasing the temperature, indicating a possibility to regenerate this kind of adsorbent by conventional method.

It is also noticed that when the concentration of DPM more than 500 ppm was prepared, fine particles of DPM was always observed. Due to a lack of information relating to the solubility of DPM in n-heptane, therefore, this work did not attempt to determine equilibrium concentration at >500 ppm. In this simple system, the adsorption isotherms approaching close to its plateau was obtained.

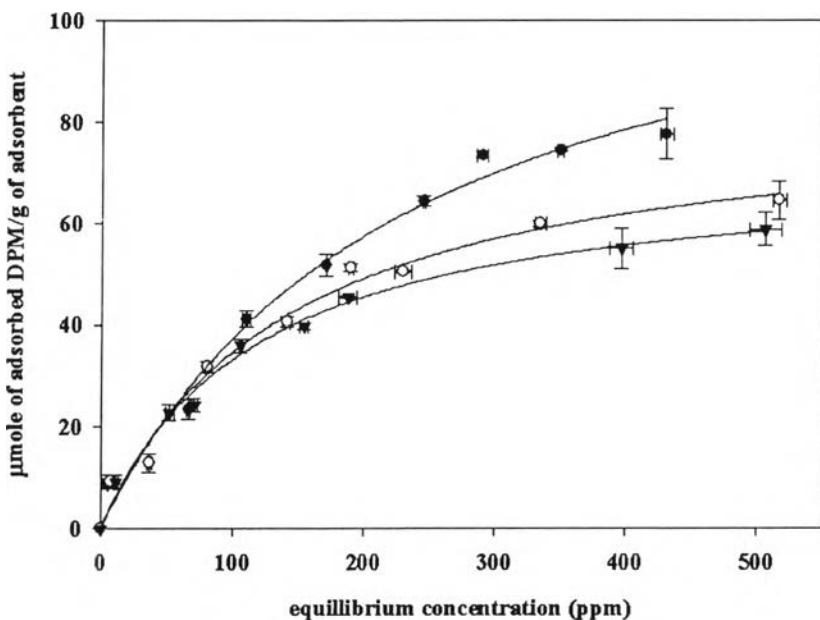


Figure 4.4 Adsorption of DPM in n-heptane at various temperatures with NaX
(● = 30°C, ○ = 40°C and ▼ = 50°C)

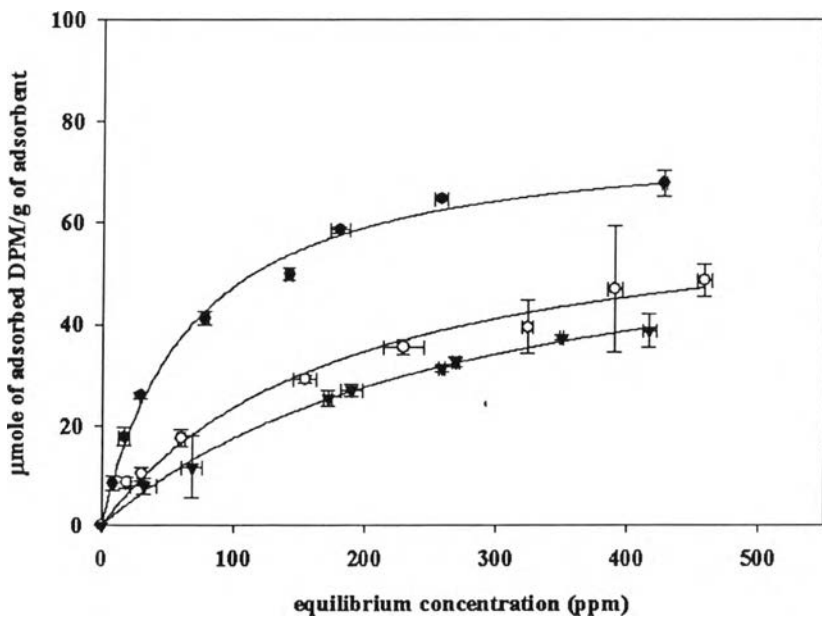


Figure 4.5 Adsorption of DPM in n-heptane at various temperatures with NaY
(● = 30°C, ○ = 40°C and ▼ = 50°C)

4.5 Effect of Alicyclic and Aromatic Hydrocarbons on DPM Adsorption

In the previous work, the experiment was done using n-heptane as simulated condensate. In fact, there are various hydrocarbons in industrial condensate. Industrially, faujasite zeolite is currently used in aromatic separation process. Therefore, the influence of aromatic hydrocarbons needs to be studied. The experiment was performed by using mixed solutions between n-heptane and other hydrocarbons separately, cyclohexane, ethylbenzene, *o*-xylene and toluene varying between 0 to 25% by mass according to the composition of heavy naphtha obtained from The Aromatic (Thailand) Public Company Limited. DPM was spiked in each solution as high as 2000 ppb. Figure 4.6 shows the influence of cyclohexane on adsorption of diphenylmercury.

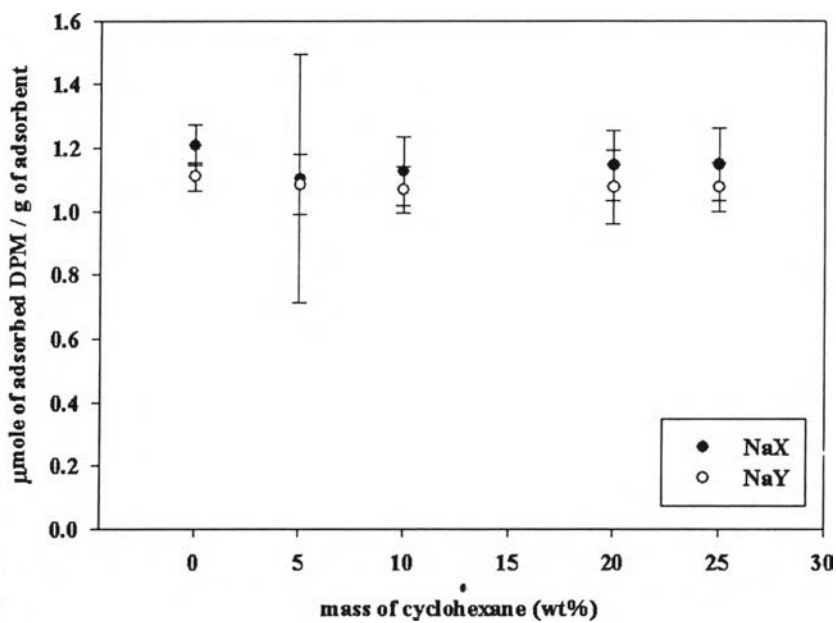


Figure 4.6 Effect of cyclohexane on adsorption of diphenylmercury (2000 ppb in n-heptane)

The result shows no influence of cyclohexane as the representative of naphthalene molecule on adsorption of DPM on either NaX or NaY.

Figure 4.7 shows little influence of ethylbenzene molecule on adsorption of DPM on both NaX and NaY.

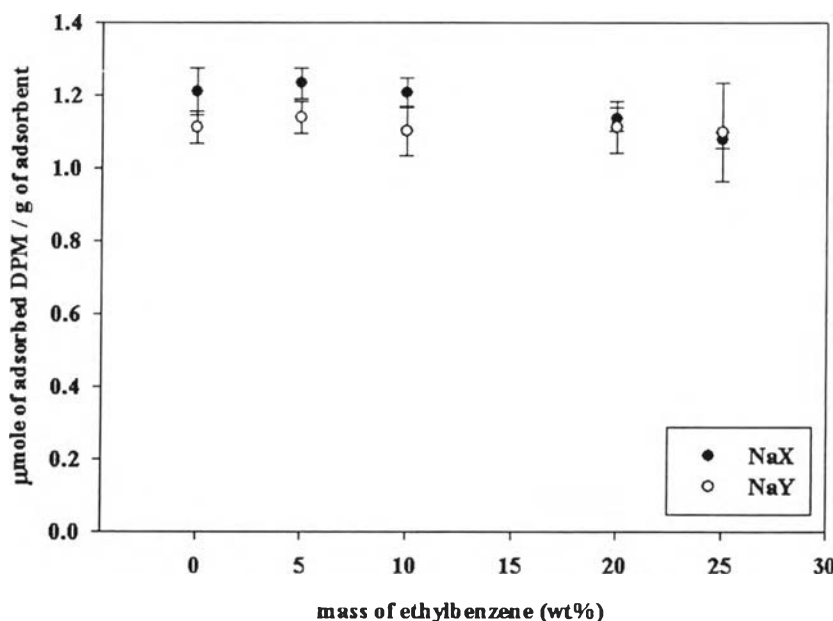


Figure 4.7 Effect of ethylbenzene on adsorption of diphenylmercury (2000 ppb in n-heptane)

Figure 4.8 shows a slight trend of *o*-xylene influence on the adsorption capacity of both NaX and NaY at 5% mass of *o*-xylene. No additional effect was observed from 10 to 25% *o*-xylene addition.

Similarly, Figure 4.9 shows the little influence of toluene. The adsorption capacity of both NaX and NaY decreased when mass of toluene increased (in the range of 5-25%).

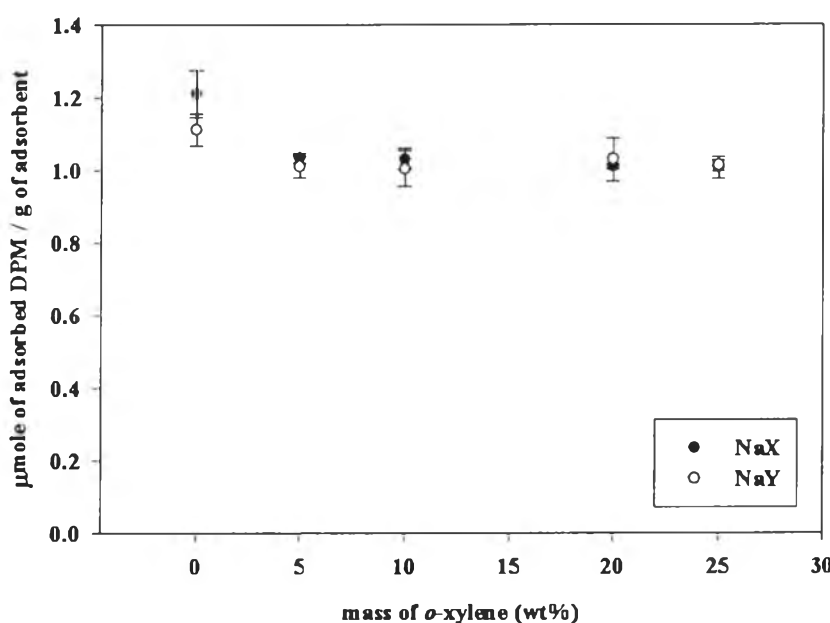


Figure 4.8 Effect of *o*-xylene on adsorption of diphenylmercury (2000 ppb in n-heptane)

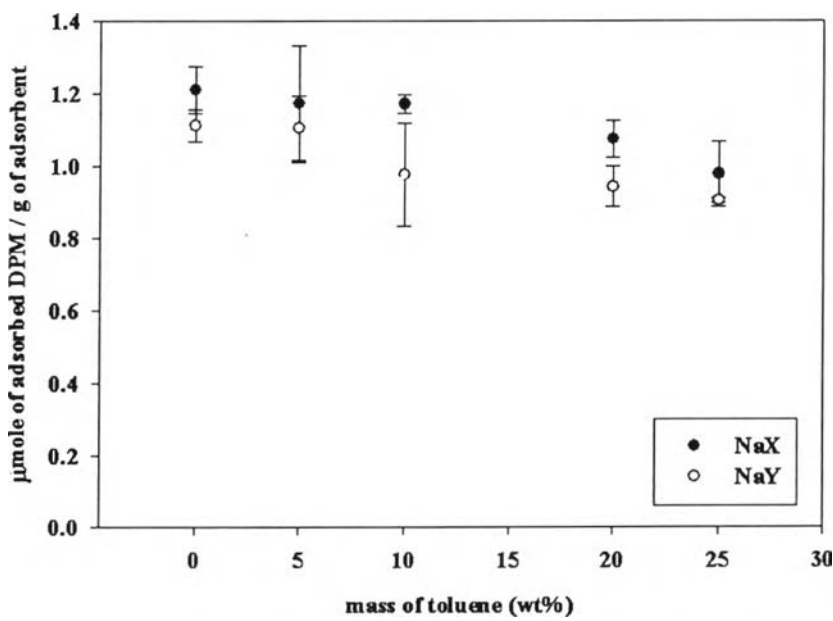


Figure 4.9 Effect of toluene on adsorption of diphenylmercury (2000 ppb in n-heptane)

122242879

Comparison of the effect of hydrocarbon type on adsorption is shown in Table 4.2. Cyclohexane, which has no π -electron showed no affinity to both NaX and NaY, in contrast with other aromatic molecules, which showed remarkable reduction of adsorbent capacity.

The aromatic molecules are able to adsorb on faujasite zeolite as revealed in many literatures, for example; Barthomeuf (1986), from Exxon Research & Engineering Company, patented the process for separating ethylbenzene from xylenes by selective adsorption by beta zeolite; Simperler (2002) studied adsorption of toluene on faujasite-type zeolites and Fitch *et al.*, (1986) reported the location of benzene in NaY zeolite by powder neutron diffraction.

The adsorption of the aromatic molecules is based on chemical bonding between its π -electron and the adsorption site (cation position) in the supercages (α -cages). In addition, there was also an evidence of the physical adsorption position in the work reported by Fitch *et al.*, (1986), who found that benzene adsorbs differently in two locations. The first benzene molecule is found in the supercage where it is bonded via its π -electron density to the sodium ion position. The second benzene molecule is held by van der Waals forces in the circular window (7.4 Å diameter) that links together neighboring supercages as shown in Figure 4.10. The four benzene molecules can rearrange and chemically adsorb in the supercage.

Table 4.2 Summary of the effect of alicyclic and aromatic hydrocarbons on adsorption of diphenylmercury

Hydrocarbons		cyclohexane	ethylbenzene	<i>o</i> -xylene	toluene
decreased capacity (%)	NaX	5.1±12	11.1±5	16.8±3	19.2±6
	NaY	2.9±6	1.1±12	8.8±4	18.5±3

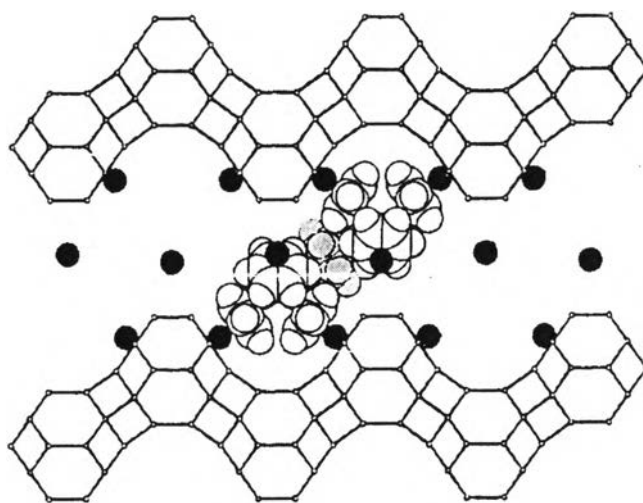


Figure 4.10 Cross-section through the interconnecting cavities of the Y zeolite, showing the Si/Al framework, the sodium ions (black circles, ionic radii), and the benzene molecules (grey molecule, van der Waals radii). Two groups of four white benzene molecules (fourth molecule obscured) each completely filling a supercage are linked through the benzene molecule (grey molecule) in the window site (Fitch *et al.*, 1986)

Therefore, the reduction of adsorption capacity of NaX and NaY found in this work could be caused by competitive adsorption of aromatic molecule which is able to adsorb chemically on adsorption site and physically on the window linked together the supercage. This finding indicates that in order to remove organomercury from liquid hydrocarbon containing high composition of aromatic with this kind of adsorbent, the competitive adsorption of aromatic molecule need to be concerned.

4.6 Adsorption Isotherm of DPM in Heavy Naphtha

The composition of treated heavy naphtha is shown in Table 4.3. In fact, this heavy naphtha cut was obtained by fractionation of raw condensate from Erawan natural gas field and passed this cut through the mercury removal unit. The major components are paraffin, naphthene and aromatic.

Table 4.3 The composition of heavy naphtha (Gas Chromatography Lab, Physics and Analysis Division, IFP, Lyon, France)

Family	% m/m	% mol/mol	% v/v
n-Paraffin	17.711	17.577	19.530
iso-Paraffin	21.416	20.615	23.464
Naphthene	35.209	35.351	34.654
Aromatic	25.663	26.457	22.352
Olefin	0.000	0.000	0.000
Total	100.000	100.000	10.000

The experiment was performed by the same procedure which was performed in section 4.4. The adsorption isotherms were performed in real heavy naphtha at the same temperature of n-heptane system, 30, 40 and 50°C. The obtained results (Figure 4.11 and Figure 4.12) show the characteristic of physical adsorption as observed in the simulated system, i.e., the higher the temperature, the lower the adsorption isotherm. However, the experiment could not be performed to reach a plateau due to human health and safety measures, as DPM is classified as a highly toxic substance, referring to the section 11 in its MSDS (Sigma-Aldrich). This substance is extremely destructive to issue of the mucous membranes and upper respiratory tract, exposure with high concentration like ppm can cause nervous system disturbances. In fact, the concentrations of mercury found in natural hydrocarbon resources normally in the range of a few ppm. To avoid personal health risks, the experiment was performed appropriately. However, the resulted adsorption isotherm is close to its plateau. By comparing these figures with Figure 4.4 and 4.5, one can see that although the adsorption behavior were quite similar, the adsorption capacity was much reduced. One important factor could come from the presence of significant amount of aromatic hydrocarbon (26.457 mol%) in heavy naphtha. The adsorption isotherm is still classified as Type I Langmuir isotherm. To differentiate between the simulated system and real system, the Langmuir adsorption model need to be applied.

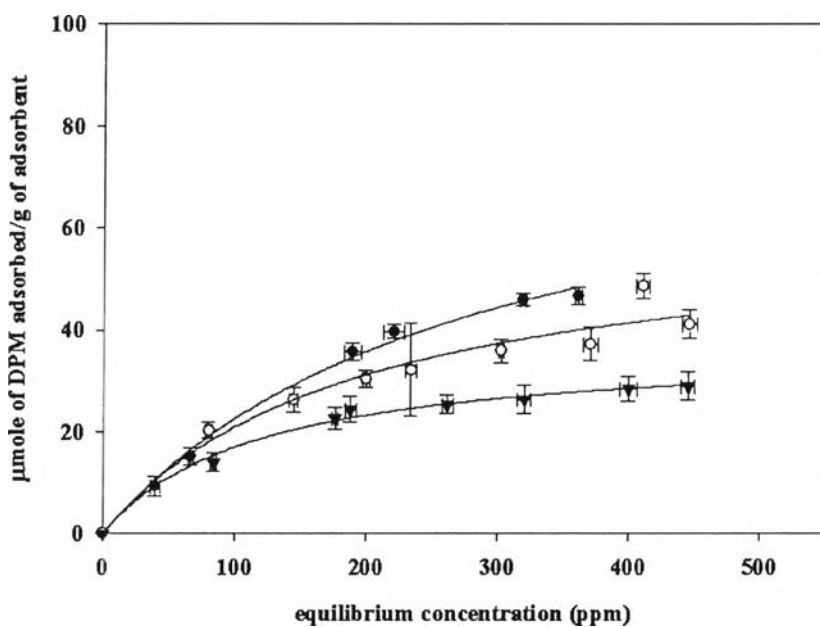


Figure 4.11 Adsorption of DPM in heavy naphtha at various temperatures with NaX
 (● = 30°C, ○ = 40°C and ▼ = 50°C)

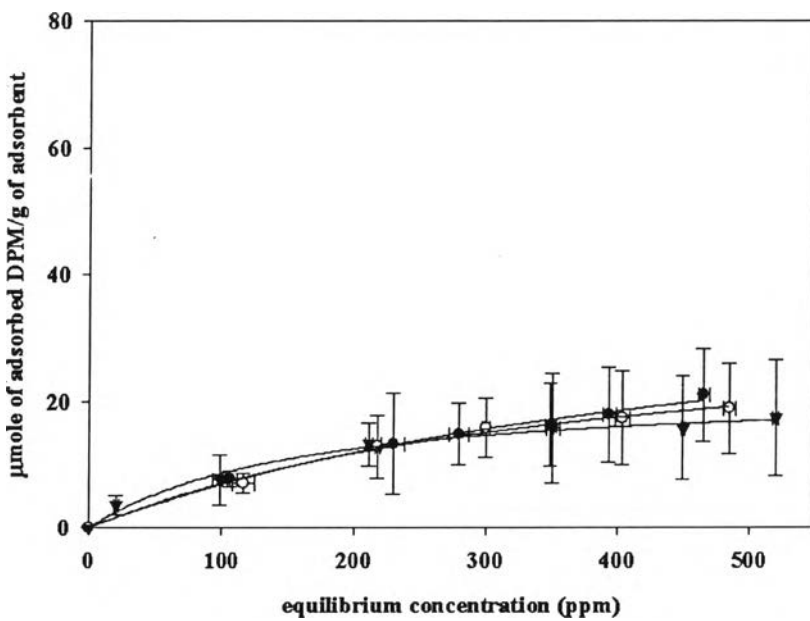


Figure 4.12 Adsorption of DPM in heavy naphtha at various temperatures with NaY
 (● = 30°C, ○ = 40°C and ▼ = 50°C)

4.7 The Langmuir Adsorption Model (Ruthven, 1984)

Referring to the text by Ruthven (1984). The model is based on the hypothesis that there is only one kind of adsorption sites that each site is equivalent to another and can adsorb only one molecule on one distinct adsorption site, and the adsorption energy is the same for all the adsorption sites.

The model determines the fraction or the ratio of the number of adsorbed molecules on the total number of molecules required for a complete monolayer, defined as θ . At the equilibrium the adsorption rate (R_{ad}) and the desorption rate (R_{de}) are equal.

$$R_{ad} = k_a(1-\theta)C \cdot L \quad (4.2)$$

$$R_{de} = k_d\theta \cdot L \quad (4.3)$$

Where C = equilibrium concentration of diphenylmercury

L = total sites for a complete monolayer

k_a & k_d = adsorption and desorption constants respectively

Therefore, the two previous equations can be rearranged as follow,

$$\theta = \frac{bC}{(1+bC)} \quad (4.4)$$

The equation can also be rewritten as follow,

$$q = \left(\frac{bC}{1+bC} \right) q_{max} \quad (4.5)$$

Where b is adsorption constant, q is the quantity of molecules adsorbed on the solid (mol/m² or mol/g of adsorbent).

Equation (4.4) can be rearranged to satisfy the first order linear relationship.

$$\frac{1}{q} = \frac{1}{q_{\max}} + \left(\frac{1}{bq_{\max}} \right) \frac{1}{C} \quad (4.6)$$

A plot between $1/C$ and $1/q$ will give an $1/q_{\max}$ as the intercept and $(1/bq_{\max})$ as the slope. The detailed correlation is shown in Appendix I. The result is shown in Table 4.4.

Table 4.4 Langmuir model parameters

Adsorbent	Temp (°C)	n-Heptane		Heavy Naphtha	
		q_{\max} (μmole/g)	b	q_{\max} (μmole/g)	b
NaX	30	123.5	2.29×10^2	85.83	2.80×10^2
	40	83.6	1.40×10^2	61.45	1.93×10^2
	50	71.86	1.16×10^2	37.01	1.18×10^2
NaY	30	77.83	6.40×10	41.0	4.79×10^2
	40	65.33	1.76×10^2	34.05	3.70×10^2
	50	64.7	2.68×10^2	22.34	1.53×10^2

The maximum capacity varies inversely with increasing temperature all in both systems. It is also noticed that at the same temperature, the adsorption capacity of heavy naphtha system was always lower than n-heptane system due to the fact that, heavy naphtha contained not only paraffin but also naphthene and aromatic hydrocarbons. As the results shown and mentioned earlier in section 4.6, the effect of cyclohexane as the representative of naphthene is negligible (5.1% for NaX and 2.9% for NaY), while the aromatic molecules like ethylbenzene, *o*-xylene and toluene significantly effected adsorption capacity. The aromatic molecule interfered adsorption of DPM by adsorbing onto both chemical and physical adsorption sites. At 30°C in n-heptane, for example, according to the industrial information provided

by IFP (personal contact) regarding to characteristic of NaY, its binder or clay quantity is around 26.7% of the adsorbent mass and the unit cell formula of NaY is known, the quantity of cages is around 2.77×10^{20} cages/g of zeolite. NaY possesses adsorption capacity as high as 77.86 $\mu\text{mole/g}$, corresponding to 0.23 molecule/ α cage.

The large reduction of adsorption capacity as shown in Figures 4.13 and 4.14 in heavy naphtha was therefore caused by the hydrocarbon matrices, in particular aromatic molecules. There are other species that also competitively adsorbed on NaX and NaY. From this point of view, it is suggested that the lower capacity in heavy naphtha system may be due to (I) complex competitive adsorption by various species in the matrix of heavy naphtha and (II) strong interaction between diphenylmercury molecule which composed of two aromatic rings and other matrix hydrocarbons.

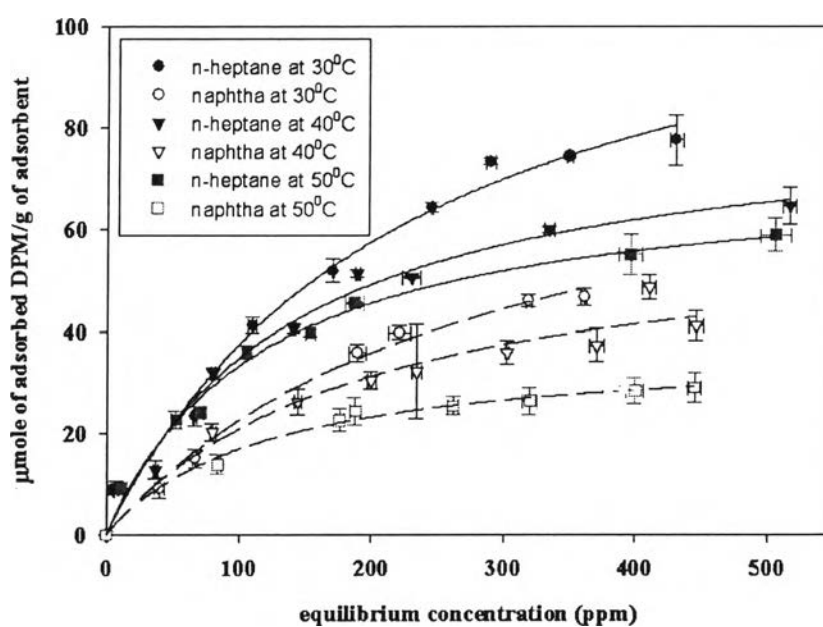


Figure 4.13 Comparison between adsorption isotherms in n-heptane and heavy naphtha by NaX (Solid symbols indicating n-heptane system and open symbols indicating heavy naphtha system)

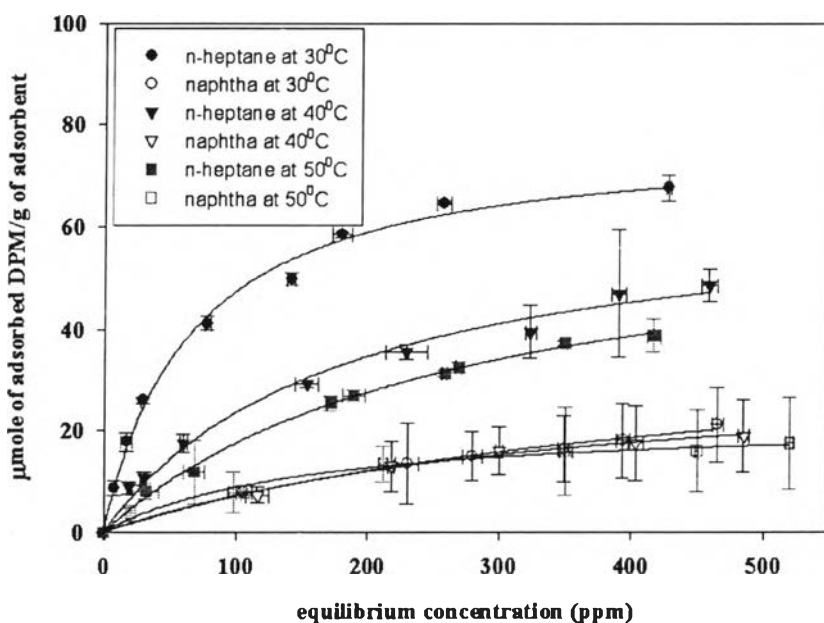


Figure 4.14 Comparison between adsorption isotherms in n-heptane and heavy naphtha by NaY (Solid symbols are n-heptane system and open symbols are heavy naphtha system)

4.8 Removal of Diphenylmercury from Heavy Naphtha in Small Pilot Unit 844

As shown by the results of batch experiment, heavy naphtha was then selected as the base hydrocarbon and spiked with 2000 ppb of DPM. Due to the time constraint, each run must be performed within an 8 hour timeframe. Referring to chapter III, therefore, 0.5 g of adsorbent was packed in the reactor. The temperature was controlled at 70°C by circulating oil bath. The pressure was controlled at 5 bars. The feed flow rate was controlled at 7 mL/min. The samples leaving the reactor were analysed by NIC mercury analyzer (SP-3D). The result from the adsorption run is shown in Figure 4.15. The outlet concentration increased rapidly after just a few minutes in the case of NaX and NaY and there was no significant adsorption on CMG273. The original concentration was recovered to around 2000 ppb at 100 minutes for NaX, 70 minutes for NaY and 40 minutes for CMG273. The higher quantity of DPM was adsorbed by NaX and NaY compared with CMG273 (CuS-

supported alumina), a small quantity of diphenylmercury was adsorbed. From this result, NaX and NaY are expected to be better adsorbents than CMG273 in order to remove organomercury from the feedstock.

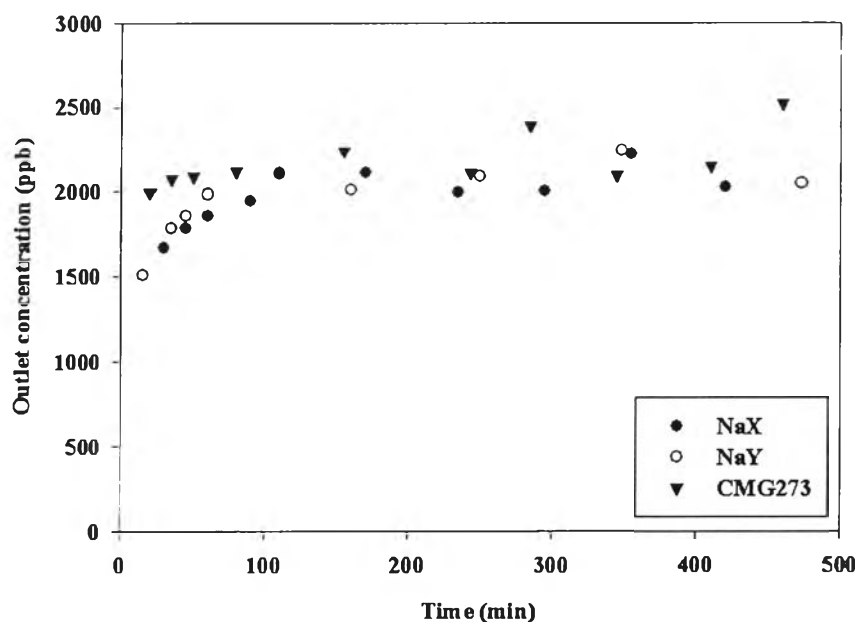


Figure 4.15 Adsorption of 2000 ppb DPM in heavy naphtha

The result from the desorption run (Figure 4.16) are as expected. Diphenylmercury rapidly desorbed from the adsorbent, especially for CMG273 after around 50 minutes. The NaX and NaY completely desorbed around 100 and 70 minutes, respectively. This confirms the characteristic of physisorption of all three adsorbents. However, from the results obtained from both batch and continuous systems, NaX is better than NaY but in the industrial operations, not only adsorption capacity need to be considered but also physical strength of the adsorbent due to the fact that, the more acidity, the more lost of physical strength to the framework. Therefore, NaY is preferred for industrial operation, and, in order to remove other species of mercury, functionalization of this kind of adsorbent is still necessary because the fact that, in liquid feedstock, metallic, inorganic and organomercury still co-exist.

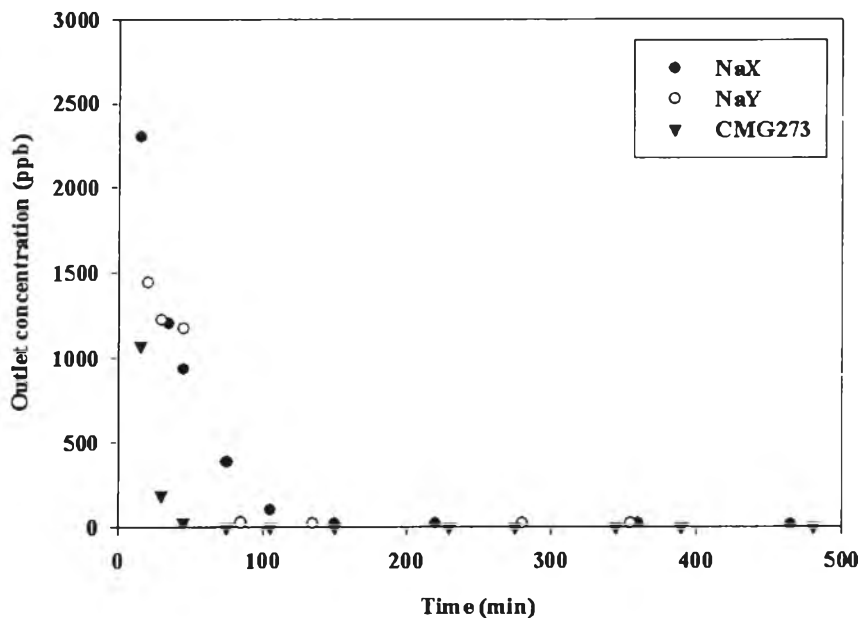


Figure 4.16 Desorption of 2000 ppb DPM in heavy naphtha

4.9 Removal of Mercury from Condensate in Small Pilot Unit 844

The condensate obtained by IFP from ATC in the year 2001 was also tested, on a trial basis. Previous analysis of feedstock shows that it contained 87% gasoline plus kerosene cut and 13% gasoil. Contaminant present in this feedstock includes 100 ppb As, 150 ppb Hg and no other metals. Nitrogen (17 ppm) and sulfur (110 ppm) can also be found (Table 4.5). It was also found that this feed contained some fine particles (personal discussion). Prior to use, analysis of Hg was made and it was found that this feed contained 180-200 ppb Hg. The experiment was performed, using the same procedure in section 4.8. The result from the adsorption run is shown in Figure 4.17. In case of NaX and NaY, the concentration was reduced to just around 150 ppb and then recovered back to its original concentration after around 200 minutes and 110 minutes respectively. The reduction of mercury to 100 ppb was obtained by CMG273 (50% removal efficiency approximately) and slightly increased with time. The previous test performed by IFP in year the 2002 indicated that CMG273 reduced Hg, by the same feed, from 150 ppb to around 70 ppb (personal

discussion). It can be said that almost 50% of the mercury in this condensate is metallic mercury referring to the reaction in section 2.7.

Table 4.5 Feed metals analysis (Elemental and Molecular Lab, Analysis Division, IFP, Lyon, France)

15 °C SpGr (g/ml)	0.7550
Mercury (µg/l)	136-156
Arsenic (µg/l)	99
Sulfur (ppm)	110
Total Nitrogen (ppm)	17
Total Oxygen (wt%)	< 0.2
Metals (mg/kg)	0
Ba	1
Ca	0
Mg	1
B	0
Zn	0
P	0
Fe	0
Cr	1
Al	0
Cu	1
Sn	0
Pb	0
V	0
Mo	0
Si	39
Na	0
Ni	0
Ti	0
Ag	0
Co	0
Mn	0

The adsorption curves of NaX and NaY indicate small amount of adsorption. The adsorption by zeolite could also be affected by aromatic fraction as shown in section 4.5 and the presence of microparticles suspending in condensate, resulting in reduction of its performance.

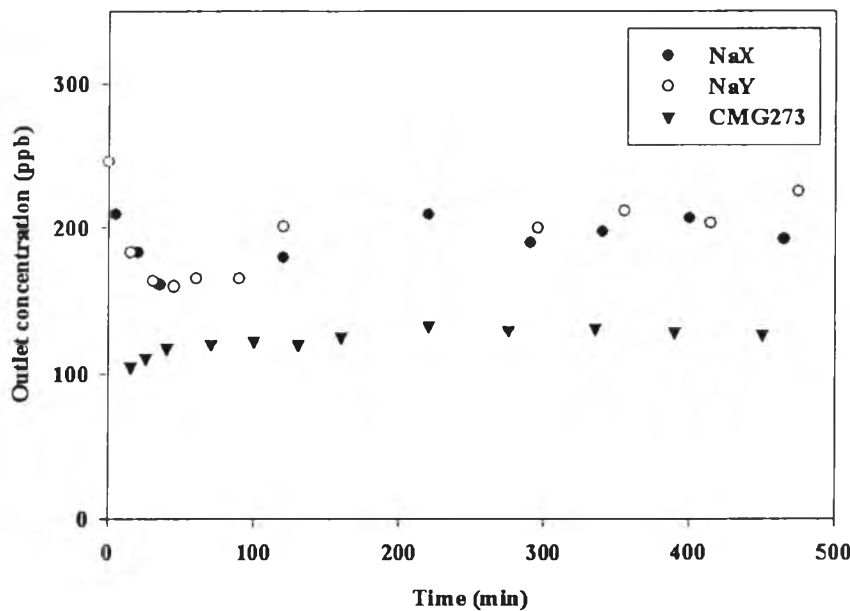


Figure 4.17 Adsorption of condensate

The desorption run was performed by flowing pure n-heptane through the packed bed after adsorption run, the conditions were held the same with section 4.8. According to the obtained result (Figure 4.18), The concentration closed to 0 ppb were observed from all three adsorbents, again, this reveals the characteristic of physisorption. NaY seems to desorb less during the first 100 minutes, but actually this might be due to the operation as Hg could accumulate resulting in higher desorption of NaY.

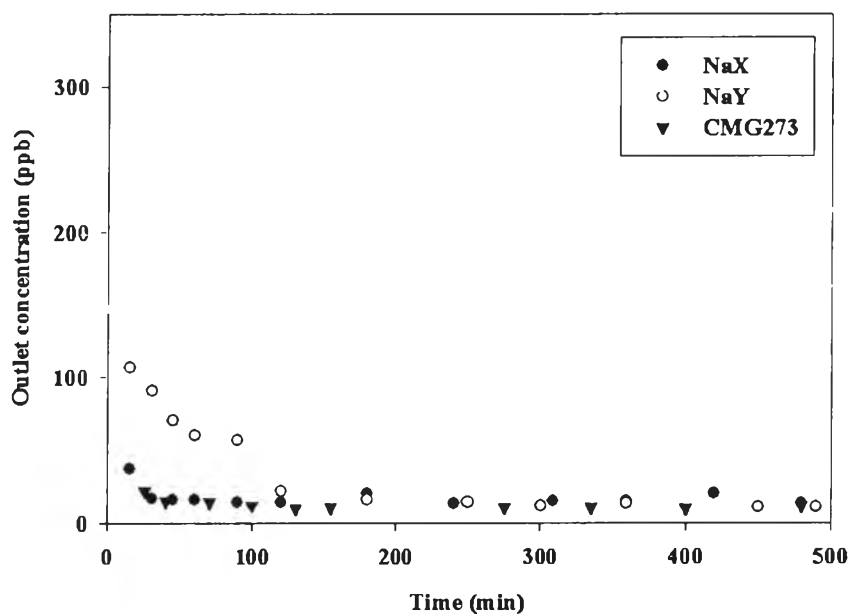


Figure 4.18 Desorption of real condensate